



Influence of pH on corrosion resistance of slippery liquid-infused porous surface on magnesium alloy

Wen-hui YAO^{1,2}, Guo-xiang ZHAN¹, Yong-hua CHEN¹, Jie QIN¹, Liang WU^{1,2},
Yan-ning CHEN¹, Jia-hao WU¹, Bin JIANG^{1,2}, Andrej ATRENS³, Fu-sheng PAN^{1,2}

1. College of Materials Science and Engineering, Chongqing University, Chongqing 400044, China;
2. National Engineering Research Center for Magnesium Alloys, Chongqing University, Chongqing 400044, China;
3. School of Mechanical and Mining Engineering, The University of Queensland, Brisbane Qld 4072, Australia

Received 26 May 2022; accepted 6 December 2022

Abstract: A slippery liquid-infused porous surface (SLIPS) was developed on the AZ31 Mg alloy to provide corrosion protection. A layered double hydroxide (LDH) was applied to providing accommodation for liquid lubricants. The electrolyte pH was adjusted to obtain the best LDH film for the development of a SLIPS. The surface morphology, surface wettability, and electrochemical behavior of the SLIPS formed at different pH values were investigated. The results indicated that the MgAl-LDH film synthesized at a pH of 10.5 had a maximum thickness of 3.51 μm to accommodate the most silicone oil, with a mass of 0.22 mg/mm^2 , which provided the best corrosion protection, with the lowest corrosion current density of $3.72 \times 10^{-9} \text{ A}/\text{cm}^2$. On the other hand, compared with the superhydrophobic surface, the SLIPS imparted better corrosion resistance for the AZ31 substrate in both electrochemical behavior and long-term immersion test. The improved corrosion resistance of the SLIPS can further accelerate the application of Mg alloys in practice.

Key words: slippery liquid-infused porous surface; electrolyte pH; corrosion resistance; surface hydrophobicity; AZ31 Mg alloy

1 Introduction

Magnesium (Mg) alloy, which has low density, high electrical conductivity, damping capacity, and good biodegradability, is one of the lightest structural engineering materials [1–3]. Therefore, Mg alloys are extremely popular in the fields of electronic communications, aerospace, military industry, and degradable biomaterials. However, the standard electrode potential of Mg is approximately -2.37 V , which leads to the unsatisfactory corrosion resistance of Mg alloys to seriously restrict their wide applications [4–7].

Different strategies have been developed to

improve the corrosion resistance of Mg alloys. Among them, surface treatment has attracted a lot of interest. Nevertheless, some surface treatment methods have disadvantages, such as high porosity of a micro-arc oxidation coating [8,9], poor degradation of chemical conversion films [10], and short-term effective protection of superhydrophobic coating [11].

Recently, a slippery liquid-infused porous surface (SLIPS), inspired by the *Nepenthes*, has received a great deal of attention in many research areas. This is because slippery liquid-infused porous (SLIPSS) can provide extremely low adhesion and possess good self-healing performance. MANNA and LYNN [12] constructed a smooth antifouling

Corresponding author: Wen-hui YAO, Tel: +86-19823476117, E-mail: yaowh2012@cqu.edu.cn;

Liang WU, E-mail: wuliang@cqu.edu.cn

DOI: 10.1016/S1003-6326(23)66335-6

1003-6326/© 2023 The Nonferrous Metals Society of China. Published by Elsevier Ltd & Science Press

SLIPS on polytetrafluoroethylene tubing. CHEN et al [13] demonstrated the effectiveness of SLIPS-modified biomedical implants to resist device-associated infection after bacterial challenge in vivo. In addition, SLIPS is also used to protect metallic substrates of Al [14], Ti [15], and steel [16] from severe corrosion. Nevertheless, the development of SLIPSs on Mg alloys was paid less attention.

Different from a superhydrophobic surface, a hierarchical structure is filled with liquid lubricant to form a SLIPS, presenting a smooth and stable liquid layer. Moreover, the liquid lubricant in the SLIPS is more stable than air pockets in the superhydrophobic coating [16,17]. That is, the preparation of SLIPS also requires rough porous structures. Layered double hydroxide (LDH) that is widely used for corrosion protection of Mg alloys, is one of the appropriate candidates to provide the desired porous structure [18,19]. In addition, LDH can carry an anionic corrosion inhibitor to further improve the corrosion resistance [20,21]. Thus, a SLIPS formed by LDH shows great potential to provide effective corrosion protection for Mg alloys [22]. However, the effect of electrolyte pH on the corrosion resistance of SLIPS based on LDH for Mg alloys has not received adequate attention and further research is urgently required.

Herein, MgAl-LDH was first synthesized on the AZ31 Mg alloy via the hydrothermal method. Then, MgAl-LDH was treated with 1H, 1H, 2H, 2H-perfluorodecyltriethoxysilane (PFDS) for low-surface-energy modification and then filled with silicone oil to form a SLIPS. In particular, the electrolyte pH for the synthesis of MgAl-LDH was changed to study the effect of pH on the corrosion resistance of SLIPS. The surface morphology, chemical composition, surface wettability, and corrosion resistance of SLIPS were studied.

2 Experimental

2.1 Preparation of SLIPS

2.1.1 Fabrication of MgAl-LDH

The AZ31 Mg alloy (with a nominal composition in wt.%: Al 2.1–3.5, Zn 0.7–1.3, Mn 0.2–1, Ca 0.04, Si 0.1, Cu 0.05, Fe <0.003, and balance Mg) was cut into specimens with sizes of 18 mm × 18 mm × 5 mm. They were gradually polished with SiC papers to 2000 grit, then washed

with ethanol and deionized water, and dried with warm air.

0.1 mol/L sodium nitrate and 0.05 mol/L aluminum nitrate were dissolved into deionized water. Then, 1 mol/L sodium hydroxide solution was slowly added into the mixed solution to adjust the pH of the electrolyte to 8.5, 9.5, 10.5, 11.5, and 12.5, respectively. Subsequently, the prepared Mg alloy specimens were immersed in corresponding electrolytes, transferred into autoclaves, and heated at 125 °C in a vacuum oven for 10 h. Finally, the AZ31 alloys with MgAl-LDH were ultrasonically cleaned in ethanol solution for 10 min and dried by a hair dryer.

2.1.2 Low-surface-energy modification

Although MgAl-LDH can provide porous microstructures to accommodate liquid lubricant for SLIPS, the MgAl-LDH is hydrophilic. Consequently, in order to prepare a SLIPS, MgAl-LDH has to be chemically modified to be hydrophobic to tightly anchor the liquid lubricant and repel the external corrosive environment. In this work, MgAl-LDH was treated using a low-surface-energy material of 1H, 1H, 2H, 2H-perfluorodecyltriethoxysilane (PFDS). Briefly, the AZ31 Mg alloy with MgAl-LDH was immersed in 0.02 mol/L PFDS in ethanol for 6 h to be superhydrophobic.

2.1.3 Lubricant infusion

The chemically modified MgAl-LDH (MgAl-LDH-PFDS) specimens were coated with dimethyl silicone oil with a viscosity of 20 mPa/s using a straw and placed in a vacuum oven for 2 h. Then, the samples were placed with an inclination angle of 10° for 2 h to remove the excess dimethyl silicone oil, obtaining the SLIPS. The schematic illustration of the preparation process is presented in Fig. 1.

2.2 Characterization

The surface and cross-sectional morphologies were characterized using a scanning electron microscope (SEM, Vega3, TESCAN SRO, Czech). The crystalline structure was analyzed by X-ray diffractometer (XRD, D/Max 2500X, Rigaku, Japan) using filtered Cu K_{α1} (0.15406 nm) as a radiation source with a scanning rate of 2 (°)/min from 5° to 80° of 2θ. The water contact angle (WCA) was measured by a SmartDrop (FEMTOFAB Co., Korea) at ambient temperature.

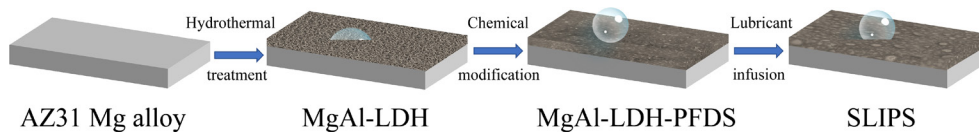


Fig. 1 Schematic illustration of preparation process for SLIPS

2.3 Electrochemical test

The anti-corrosion performance was evaluated using an electrochemical workstation (PARSTAT 4000 A, Princeton, USA) in a 3.5 wt.% NaCl solution at room temperature, including polarization curves and electrochemical impedance spectroscopy (EIS). The measurement was carried out in a three-electrode cell with a platinum (Pt) electrode as the counter electrode, a saturated calomel electrode (SCE) as the reference electrode, and a specimen with a working area of 1 cm² as the working electrode. All measurements were based on the open circuit potential. The scanning rate was 1 mV/s, and the scanning range was ± 500 mV regarding the open circuit potential. The Versastudio software was used to collect and record the experimental data, and the ZSimpWin software was used to fit the data.

2.4 Hydrogen evolution test

The immersion of Mg alloys in 3.5 wt.% NaCl solution can cause hydrogen evolution reaction, dissolving and releasing hydrogen. Therefore, the corrosion rate of Mg alloys can be estimated by measuring the hydrogen evolution rate, and its corrosion resistance can be evaluated. The schematic diagram illustrating the hydrogen evolution test is presented in Fig. 2. The liquid level was recorded every 12 h during the hydrogen evolution test [23].

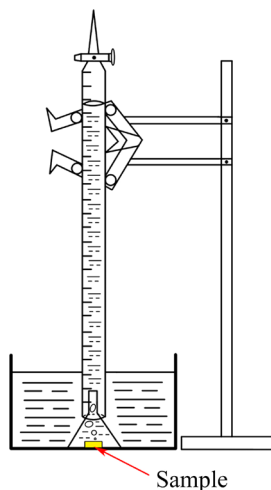


Fig. 2 Schematic diagram of hydrogen collection device

3 Results and discussion

3.1 Surface and cross-sectional morphology

Figure 3 shows the surface morphology of MgAl-LDH formed at different pH values on the AZ31 Mg alloy. The typical nano-sheet structures of the MgAl-LDH are detected on all samples after hydrothermal treatment; thus, the MgAl-LDH can be synthesized on AZ31 Mg alloy at different pH values ranging from 8.5 to 12.5. However, when the pH is 8.5, there is a relatively deep crack on the surface (Fig. 3(a)), indicating that the AZ31 Mg alloy was severely damaged during the hydrothermal reaction. The occurrence of cracks was attributed to the substantial stresses, resulting from the formation of a large number of reaction products that were accumulated unevenly [24,25]. In addition, the MgAl-LDH film did not completely cover the whole surface of the AZ31 Mg alloy. Therefore, the pH of 8.5 is not an appropriate experimental condition for the synthesis of MgAl-LDH in this work.

According to Figs. 3(b)–(e), the thickness of the nanosheet increases with increasing pH, and the density of the nanosheets decreases. Although there were no cracks when the pH increased to 9.5, the thickness of the nanosheet was still thin. Thus, the formed MgAl-LDH film maybe was not strong enough to be applied in practice. When the pH was 11.5 and 12.5, the thickness of the nanosheets increased slightly, but the density decreased significantly, resulting in excessively high porosity.

The cross-sectional SEM images of MgAl-LDH films produced at different pH values are shown in Fig. 4. Their thicknesses were respectively 1.55, 3.16, 3.51, 2.41, and 1.90 μm when the pH was 8.5, 9.5, 10.5, 11.5, and 12.5. Therefore, the thickness of MgAl-LDH films increased first, attained the maximum when the pH was 10.5, and then decreased with increasing pH. This further proved that the electrolyte pH played a significant effect on the growth of MgAl-LDH films.

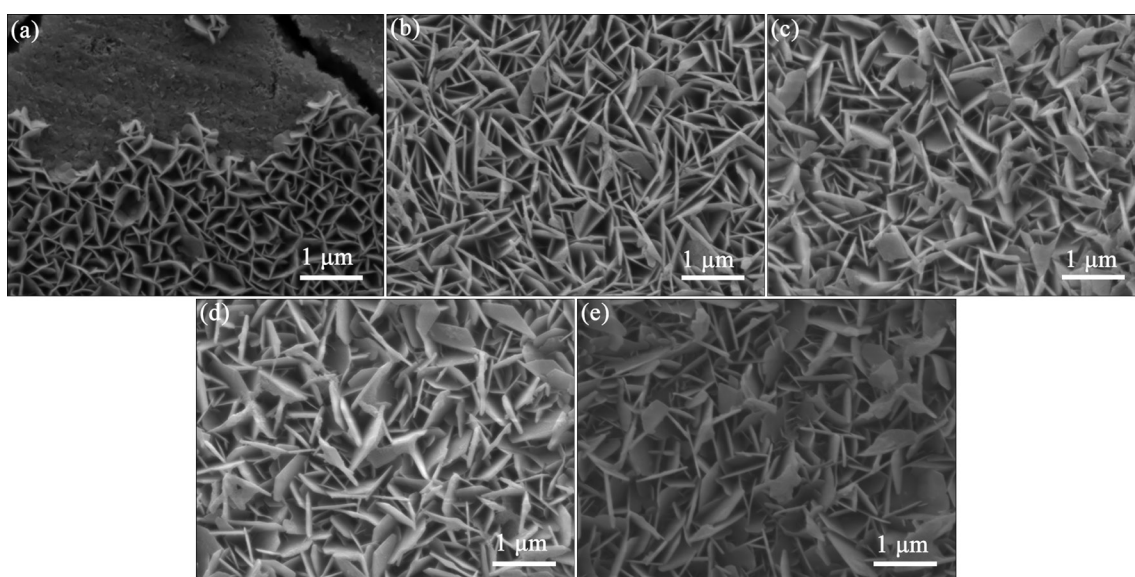


Fig. 3 SEM images of surface morphology of MgAl-LDH formed at different pH values: (a) 8.5; (b) 9.5; (c) 10.5; (d) 11.5; (e) 12.5

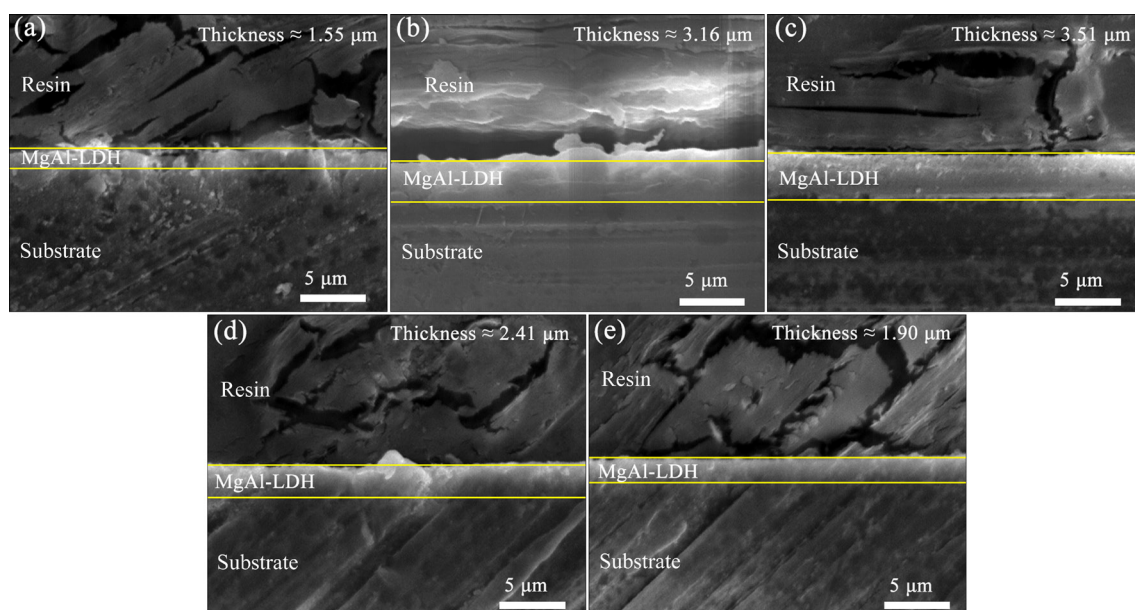


Fig. 4 SEM images of cross-sectional morphology of MgAl-LDH formed at different pH values: (a) 8.5; (b) 9.5; (c) 10.5; (d) 11.5; (e) 12.5

Figure 5(a) displays the variation of silicone oil mass with electrolyte pH. Consistent with the SEM images (Figs. 3 and 4), the MgAl-LDH film synthesized at a pH of 10.5 can accommodate the most silicone oil, with a mass of 0.22 mg/mm^2 . Therefore, comprehensively considering the thickness and density of the nanosheets, film thickness, and the capacity to accommodate silicone oil, the electrolyte pH of 10.5 was the best condition for the synthesis of MgAl-LDH film for a SLIPS.

Moreover, Fig. 5(b) shows the SEM image of the SLIPS based on the MgAl-LDH film formed at a pH of 10.5. Compared to Fig. 3(c), the nanosheet structure of the MgAl-LDH becomes inconspicuous, and the gaps among numerous nanosheets are filled with liquid, presenting a stable liquid layer. Therefore, the dimethyl silicone oil can be stably placed at the nanoporous structures of the MgAl-LDH to effectively prevent the invasion of corrosive species to increase corrosion resistance.

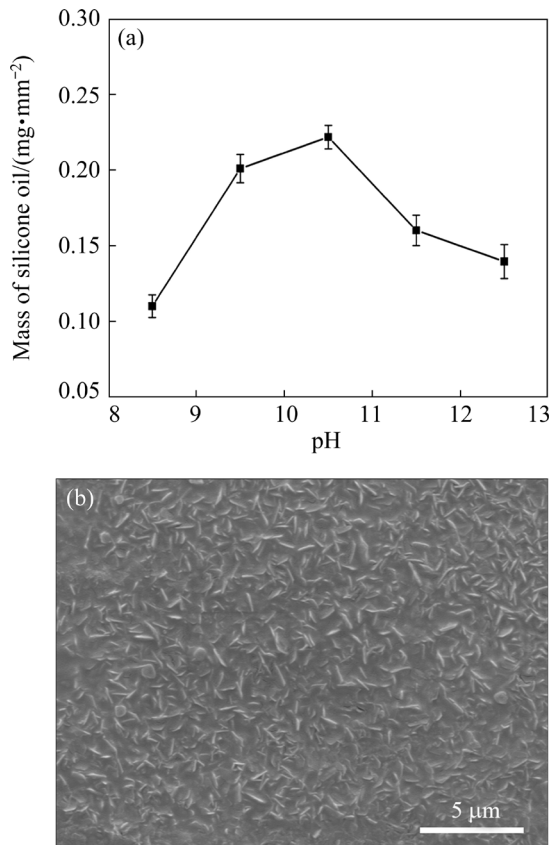


Fig. 5 Variation of silicone oil mass with electrolyte pH (a), and SEM image of surface morphology of SLIPS developed with MgAl-LDH formed at pH of 10.5 (b)

3.2 Surface chemistry

Figure 6 shows XRD patterns of MgAl-LDH films synthesized at different electrolyte pH values. The typical peaks corresponding to the (003) and (006) reflection planes of the LDH can be detected

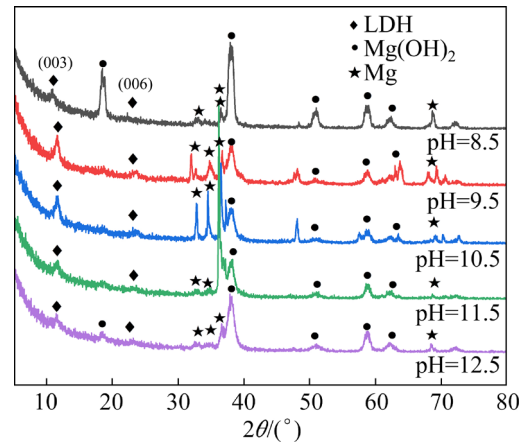


Fig. 6 XRD patterns of MgAl-LDH formed at different pH values

even when the pH is 8.5, indicating that MgAl-LDH films were synthesized on all AZ31 Mg alloy samples, which was consistent with the results in Figs. 3 and 4.

3.3 Surface wettability

The optical photographs of water droplets on MgAl-LDH prepared at different pH values are shown in Figs. 7(a)–(e). The WCAs were respectively 20.7°, 52.1°, 50.8°, 55.7°, and 56.5° when the pH was 8.5, 9.5, 10.5, 11.5, and 12.5, showing the surface hydrophilicity of MgAl-LDH. The relatively low WCA of the MgAl-LDH film at a pH of 8.5 was mainly related to the large cracks on its surface. After the chemical modification by PFDS, the as-prepared sample of MgAl-LDH-PFDS exhibited surface superhydrophobicity, with a

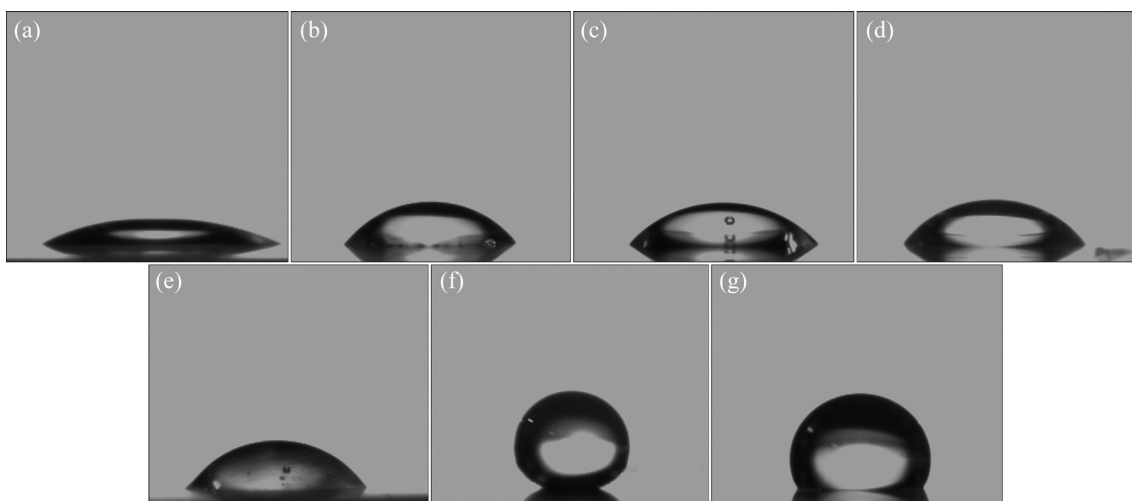


Fig. 7 Optical photographs of water droplets on MgAl-LDH films formed at different pH values: (a) 8.5; (b) 9.5; (c) 10.5; (d) 11.5; (e) 12.5; (f) MgAl-LDH-PFDS; (g) SLIPS formed by MgAl-LDH film at pH of 10.5

WCA of 150.5° , where the water droplet presented like a ball. Furthermore, after the liquid lubricant of dimethyl silicone oil was infused into the porous structure of the MgAl-LDH, the WCA decreased to 117.8° in Fig. 7(g). The water-immiscible lubricant occupied the nanopores and pushed out the trapped air, resulting in the contact interface changing from the water–air–solid to water–liquid–solid [26]. Although the WCA decreased compared with the MgAl-LDH-PFDS, the SLIPS still showed surface hydrophobicity.

3.4 Electrochemical behavior

Figure 8 shows the Tafel curves of different samples. Generally, a lower corrosion current density indicates better chemical stability and corrosion protection [24]. The AZ31 Mg alloy exhibits the highest corrosion current density ($6.75 \times 10^{-5} \text{ A/cm}^2$), showing extremely poor corrosion resistance. The corrosion current density gradually decreased after the formation of MgAl-LDH ($3.33 \times 10^{-7} \text{ A/cm}^2$), MgAl-LDH-PFDS ($5.06 \times 10^{-8} \text{ A/cm}^2$), and SLIPS ($3.72 \times 10^{-9} \text{ A/cm}^2$). Therefore, the corrosion resistance was gradually improved by these appropriate treatments. In comparison with the bare AZ31 Mg alloy, the corrosion current density of the SLIPS was decreased by about four orders of magnitude, indicating that the formed SLIPS by MgAl-LDH significantly increased the corrosion resistance. Moreover, Fig. 8(b) compares the corrosion resistance among SLIPSs based on MgAl-LDH films synthesized at different electrolyte pH. As expected, the SLIPS prepared with MgAl-LDH film at a pH of 10.5 exhibited the lowest corrosion current density of $3.72 \times 10^{-9} \text{ A/cm}^2$. This is consistent with its optimal surface morphology, the largest film thickness, and capacity to contain the most silicone oil. Therefore, the pH of 10.5 is the best condition for the synthesis of MgAl-LDH to form a SLIPS with the best corrosion protection for AZ31 Mg alloy.

The EIS was measured to explore the corrosion protection mechanism. The impedance modulus ($|Z|$) value at 10 mHz approximately corresponds to the impedance of specimens to predict corrosion resistance. Therefore, samples with higher $|Z|$ at 10 mHz have better corrosion resistance. According to Fig. 9, the corrosion resistance of SLIPSs is ranked as follows:

pH 10.5 > pH 9.5 > pH 11.5 > pH 12.5 > pH 8.5. This is consistent with Tafel curves, and the SLIPS synthesized at a pH of 10.5 presents the best corrosion protection for the AZ31 substrate.

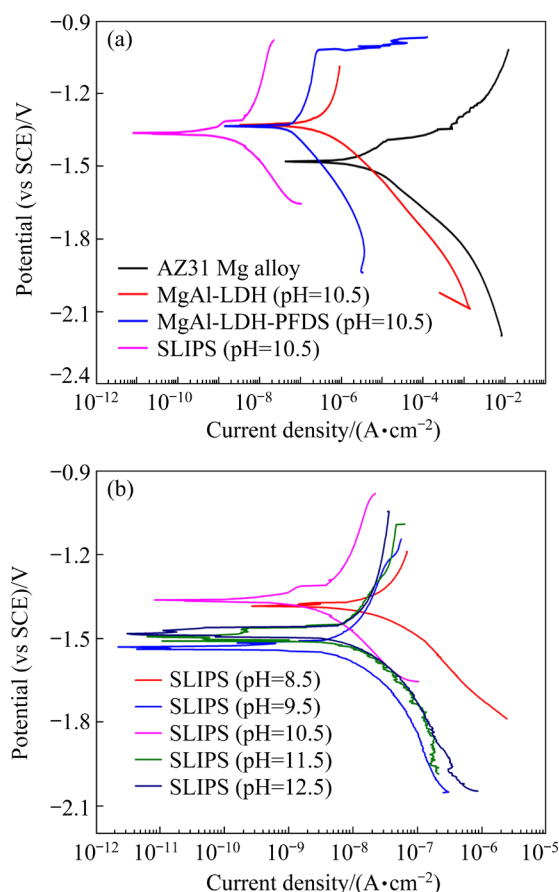


Fig. 8 Tafel curves of AZ31 Mg alloy, MgAl-LDH, MgAl-LDH-PFDS, and SLIPS formed at pH of 10.5 (a), and SLIPS formed by MgAl-LDH developed at different pH values (b)

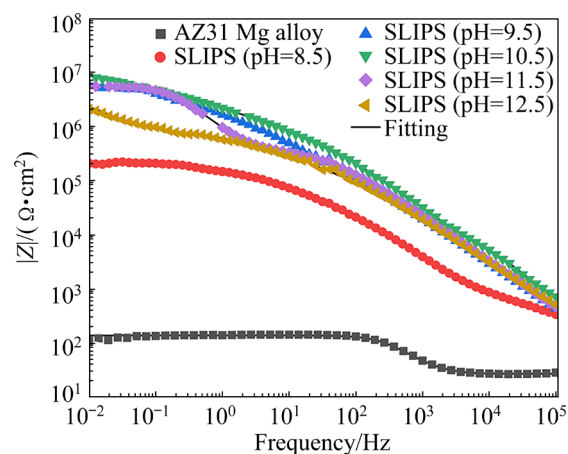


Fig. 9 Bode plots of impedance modulus of $|Z|$ vs frequency for bare AZ31 Mg alloy substrate and SLIPSs formed at different pH values

As a representative of SLIPS samples, the SLIPS developed at a pH of 10.5 was further investigated to compare the electrochemical performances among different treatment processes, with the results as presented in Fig. 10. Figure 10(a) shows that the impedance modulus $|Z|$ decreases in the order of SLIPS > MgAl-LDH-PFDS > MgAl-LDH > AZ31 Mg alloy, consistent with Nyquist results as displayed in Fig. S1 (Supporting Information). This further confirmed that each preparation step of SLIPS was beneficial to the improvement of corrosion resistance of AZ31 Mg alloys.

The equivalent circuits (Figs. 10(c) and (d)) were obtained by fitting the EIS curves. Ideal capacitors cannot analyze the interfacial process of charge transfer due to the inhomogeneity of the films. Therefore, the constant phase elements (CPE) were introduced to characterize the non-ideal capacitive behavior of the specimens. There are three time constants for the SLIPS, with an equivalent circuit of $R_{\text{sol}}(CPE_{\text{oil}}(R_{\text{oil}}(CPE_{\text{LDH}}(R_{\text{LDH}}(CPE_{\text{dl}}R_{\text{ct}}))))$, where R_{sol} stands for the solution resistance, CPE_{oil} and R_{oil} are the capacitance and resistance of the liquid layer of silicone oil in the SLIPS, CPE_{LDH} and R_{LDH} are the capacitance and resistance of LDH, and CPE_{dl} and R_{ct} refer to the

capacitance and charge transfer resistance at the Mg alloy/solution interface. In contrast, the MgAl-LDH film only has two time constants, without sealing post-treatment of silicone oil. Overall, owing to the existence of the liquid layer in the SLIPS, it presented the best corrosion protection for the underlying AZ31 alloy.

3.5 Hydrogen evolution

Figure 11 shows the variation of hydrogen evolution volume with the immersion time of the samples. The hydrogen evolution volume of the MgAl-LDH was the fastest, and all the liquid was depleted in the titration tube after only 192 h. In contrast, the hydrogen evolution volume highly decreased after the low-surface-energy modification and infusion of silicone oil. The MgAl-LDH-PFDS coating can repel the corrosive media by the fixed tiny air pockets at the solid-liquid interface. However, during the service, the air will be gradually consumed, so that the corrosive ions will be penetrated [27]. Therefore, after immersion for about 25 h, its hydrogen evolution volume began to highly increase. Especially, the hydrogen evolution volume of the SLIPS was the lowest, further indicating the best corrosion resistance and stability of SLIPS in this work, which was consistent with

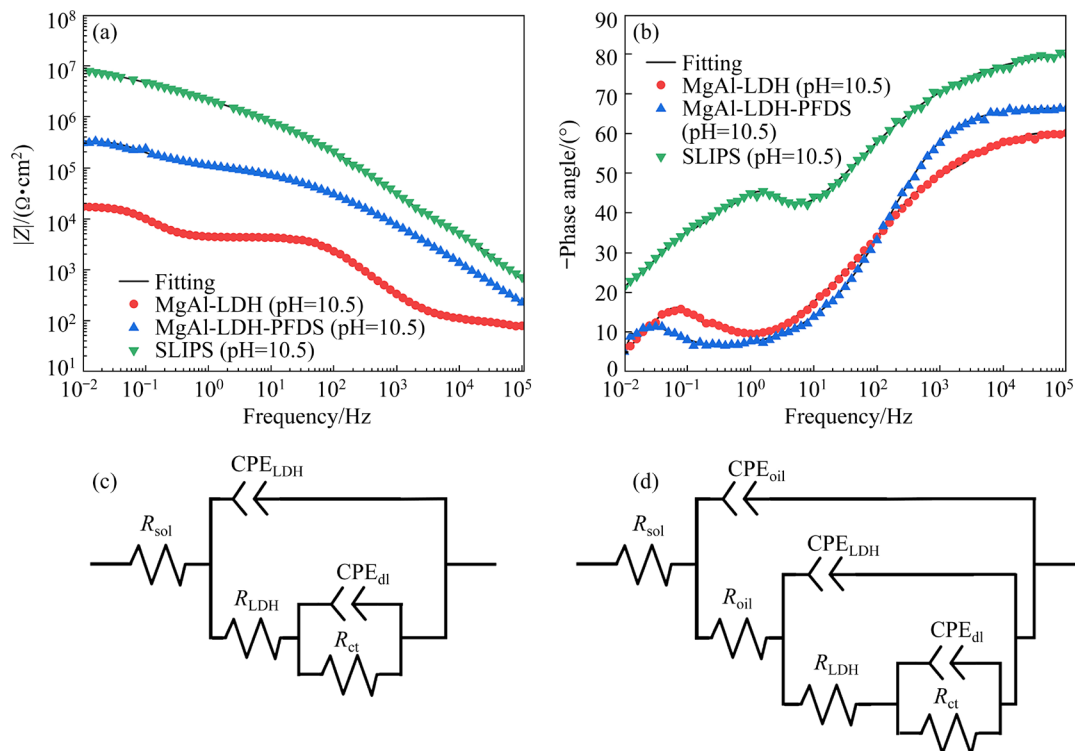


Fig. 10 Bode plots of impedance modulus $|Z|$ (a) and phase angle vs frequency (b) for MgAl-LDH, MgAl-LDH-PFDS and SLIPS formed at electrolyte pH of 10.5, and equivalent circuit models for MgAl-LDH (c) and SLIPS (d)

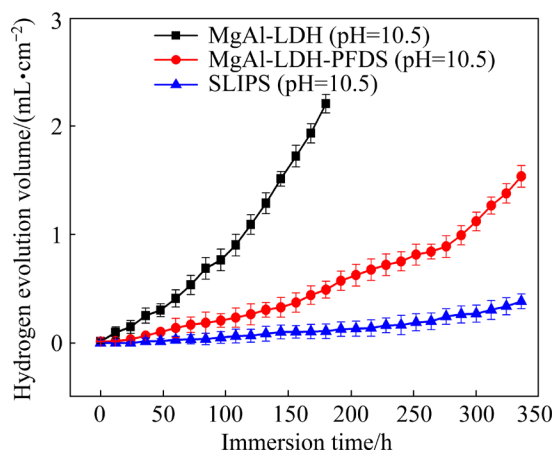


Fig. 11 Variation of hydrogen evolution volume with immersion time in 3.5 wt.% NaCl for MgAl-LDH, MgAl-LDH-PFDS, and SLIPS formed at pH of 10.5

the Tafel curves and EIS results. However, the hydrogen evolution volume of the SLIPS slightly increased with increasing immersion time, which may be due to the leakage of silicone oil during the long-term immersion [28]. Nevertheless, the SLIPS can still provide the best corrosion resistance.

3.6 Analysis of corrosion resistance mechanism

The high-density stacked MgAl-LDH nanosheets successfully form a physical barrier [29,30]. However, there are tiny pores and cracks inside, resulting in insufficient physical protection ability, as shown in Figs. 12(a) and (c). Nonetheless, the loose and porous structure of MgAl-LDH provides the necessary conditions for the injection of liquid lubricants after low-surface-energy modification (Fig. 12(b)). The injection of liquid lubricants into defects such as pores and cracks can provide a more complete physical barrier. Therefore, the invasion of corrosive solutions can be significantly restricted. In addition, the liquid layer of silicone oil is

electrically insulated, limiting electron transfer and greatly slowing down the corrosion rate. On the other hand, the SLIPS possesses self-healing performance, due to the fluidity of the liquid lubricant. Thus, when its surface is damaged, the lubricant can spontaneously flow to self-repair the defects (Fig. 12(d)) [26,31]. Furthermore, as shown in Fig. 12(e), the corrosive media of Cl^- ions can be gradually entrapped in the interlayer of MgAl-LDH and the corrosion inhibitor of anion NO_3^- is simultaneously released into the NaCl solution, owing to the good ion-exchange characteristic of LDH [32–35]. Therefore, SLIPSs can effectively improve the corrosion resistance of AZ31 alloys by providing an excellent physical barrier and corrosion inhibition.

4 Conclusions

(1) SLIPSs were successfully developed on AZ31 Mg alloys by infusion of silicone oil into the nano porous MgAl-LDH film. In particular, the MgAl-LDH was synthesized using electrolytes at different pH values.

(2) Except for a pH of 8.5, MgAl-LDH grew well on the AZ31 Mg alloy, with numerous nanosheets distributed perpendicularly, providing an appropriate nanocontainer to accommodate the silicone oil.

(3) In comparison with the bare AZ31 Mg alloy, the development of the protective coating significantly improved the corrosion resistance. Especially, when the pH was 10.5, the formed SLIPS showed the best corrosion resistance, with the lowest corrosion current density of $3.72 \times 10^{-9} \text{ A/cm}^2$. This was mainly related to the high uniformity and thickness of the MgAl-LDH to form a stable liquid layer.

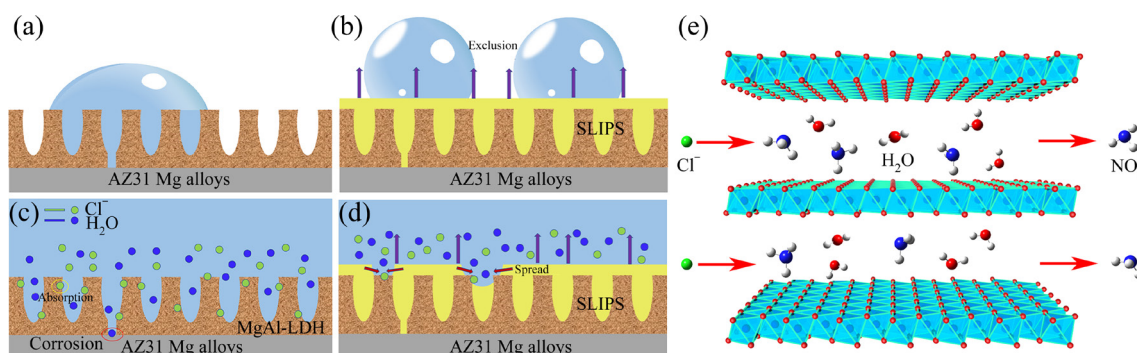


Fig. 12 Schematic diagram illustrating corrosion resistance mechanism of MgAl-LDH film (a, c, e) and SLIPS (b, d)

(4) The SLIPS presented better corrosion resistance than MgAl-LDH and the superhydrophobic surface of MgAl-LDH-PFDS in both electrochemical and long-term immersion tests, indicating effective and reliable sealing by the stable liquid layer.

Acknowledgments

This work was supported by the Chongqing Municipal Human Resources and Social Security Bureau, China (No. cx2022098), the National Natural Science Foundation of China (No. 52001036), and China Postdoctoral Science Foundation (Nos. 2022T150767, 2021M693708).

Supporting Information

Supporting Information in this paper can be found at: http://tmsc.csu.edu.cn/download/06-p3309-2022-0616-Supporting_information.pdf.

References

- [1] JIANG Bin, DONG Zhi-hua, ZHANG Ang, SONG Jiang-feng, PAN Fu-sheng. Recent advances in micro-alloyed wrought magnesium alloys: Theory and design [J]. Transactions of Nonferrous Metals Society of China, 2022, 32: 1741–1780.
- [2] TAYLOR S, WEST G D, MOGIRE E, TANG F, KOTADIA H R. Superplastic forming characteristics of AZ41 magnesium alloy [J]. Transactions of Nonferrous Metals Society of China, 2021, 31: 648–654.
- [3] SIAHSARANI A, FARAJI G. Processing and characterization of AZ91 magnesium alloys via a novel severe plastic deformation method: Hydrostatic cyclic extrusion compression (HCEC) [J]. Transactions of Nonferrous Metals Society of China, 2021, 31: 1303–1321.
- [4] WU Guo-hua, WANG Cun-long, SUN Ming, DING Wen-jiang. Recent developments and applications on high-performance cast magnesium rare-earth alloys [J]. Journal of Magnesium and Alloys, 2021, 9: 1–20.
- [5] GRGUR B N, JUGOVIĆ B Z, GVOZDENOVIĆ M M. Influence of chloride ion concentration on initial corrosion of AZ63 magnesium alloy [J]. Transactions of Nonferrous Metals Society of China, 2022, 32: 1133–1143.
- [6] DAVOODI F, ATAPOUR M, BLAWERT C, ZHELUDKEVICH M. Wear and corrosion behavior of clay containing coating on AM 50 magnesium alloy produced by aluminate-based plasma electrolytic oxidation [J]. Transactions of Nonferrous Metals Society of China, 2021, 31: 3719–3738.
- [7] LI Yang, SHI Zhi-ming, CHEN Xing-rui, ATRENS A. Anodic hydrogen evolution on Mg [J]. Journal of Magnesium and Alloys, 2021, 9: 2049–2062.
- [8] ATRENS A, SHI Zhi-ming, MEHREEN S U, JOHNSTON S, SONG Guang-ling, CHEN Xian-hua, PAN Fu-sheng. Review of Mg alloy corrosion rates [J]. Journal of Magnesium and Alloys, 2020, 8: 989–998.
- [9] ZAHEDI ASL V, CHINI S F, ZHAO Jing-mao, PALIZDAR Y, SHAKER M, SADEGHI A. Corrosion properties and surface free energy of the ZnAl LDH/rGO coating on MAO pretreated AZ31 magnesium alloy [J]. Surface and Coatings Technology, 2021, 426: 127764.
- [10] ZHANG Jia-lei, GU Chang-dong, TU Jiang-ping. Robust slippery coating with superior corrosion resistance and anti-icing performance for AZ31B Mg alloy protection [J]. ACS Applied Materials & Interfaces, 2017, 9: 11247–11257.
- [11] SAJI V S. Recent progress in superhydrophobic and superamphiphobic coatings for magnesium and its alloys [J]. Journal of Magnesium and Alloys, 2021, 9: 748–778.
- [12] MANNA U, LYNN D M. Fabrication of liquid-infused surfaces using reactive polymer multilayers: Principles for manipulating the behaviors and mobilities of aqueous fluids on slippery liquid interfaces [J]. Advanced Materials, 2015, 27: 3007–3012.
- [13] CHEN Jia-xuan, HOWELL C, HALLER C A, PATEL M S, AYALA P, MORAVEC K A, DAI E B, LIU Li, SOTIRI I, AIZENBERG M, AIZENBERG J, CHAIKOF E L. An immobilized liquid interface prevents device associated bacterial infection in vivo [J]. Biomaterials, 2017, 113: 80–92.
- [14] ZHANG Mei-ling, CHEN Rong-rong, LIU Qi, LIU Jing-yuan, YU Jing, SONG Da-lei, LIU Pei-li, GAO Liang-tian, WANG Jun. Long-term stability of a liquid-infused coating with anti-corrosion and anti-icing potentials on Al alloy [J]. Chem Electro Chem, 2019, 6: 3911–3919.
- [15] WANG Yan-jun, ZHAO Wen-jie, WU Wen-ting, WANG Chun-ting, WU Xue-dong, XUE Qun-ji. Fabricating bionic ultraslippery surface on titanium alloys with excellent fouling-resistant performance [J]. ACS Applied Bio Materials, 2019, 2: 155–162.
- [16] PRADO L, ANASTASIOU E, VIRTANEN S. Corrosion behavior of a slippery liquid infused porous surface on anodized stainless steel [J]. Materials Letters, 2021, 296: 129892.
- [17] YAO Wen-hui, WU Liang, SUN li-dong, JIANG Bin, PAN Fu-sheng. Recent developments in slippery liquid-infused porous surface [J]. Progress in Organic Coatings, 2022, 166: 106806.
- [18] GONZALEZ RODRIGUEZ P, de RUITER M P, WIJNANDS T, TEN ELSHOF J E. Porous layered double hydroxides synthesized using oxygen generated by decomposition of hydrogen peroxide [J]. Scientific Reports, 2017, 7: 481.
- [19] CHEN Jun, SONG Ying-wei, SHAN Da-yong, HAN En-hou. In situ growth of Mg–Al hydrotalcite conversion film on AZ31 magnesium alloy [J]. Corrosion Science, 2011, 53: 3281–3288.
- [20] ZENG Rong-chang, LIU Zhen-guo, ZHANG Fen, LI Shuo-qi, CUI Hong-zhi, HAN En-hou. Corrosion of molybdate intercalated hydrotalcite coating on AZ31 Mg alloy [J]. Journal of Materials Chemistry A, 2014, 2: 13049–13057.
- [21] YAO Wen-hui, CHEN Yong-hua, WU Liang, JIANG Bin, PAN Fu-sheng. Preparation of slippery liquid-infused porous surface based on MgAlLa-layered double hydroxide for effective corrosion protection on AZ31 Mg alloy [J]. Journal of the Taiwan Institute of Chemical Engineers, 2022, 131: 104176.

- [22] YAO Wen-hui, CHEN Yong-hua, WU Liang, ZHANG Ji-kai, PAN Fu-sheng. Effective corrosion and wear protection of slippery liquid-infused porous surface on AZ31 Mg alloy [J]. Surface and Coatings Technology, 2022, 429: 127953.
- [23] SONG Guang-ling, ATRENS A., STJOHN D. An hydrogen evolution method for the estimation of the corrosion rate of magnesium alloys [J]. Magnesium Technology, 2001, 255–262.
- [24] WU Yu-long, WU Liang, YAO Wen-hui, JIANG Bin, WU Jia-hao, CHEN Yan-ning, CHEN Xiao-bo, ZHAN Qin, ZHANG Gen, PAN Fu-sheng. Improved corrosion resistance of AZ31 Mg alloy coated with MXenes/MgAl-LDHs composite layer modified with yttrium [J]. Electrochimica Acta, 2021, 374: 137913.
- [25] BLAWERT C., DIETZEL W., GHALI E., SONG Guang-ling. Anodizing treatments for magnesium alloys and their effect on corrosion resistance in various environments [J]. Advanced Engineering Materials, 2006, 8: 511–533.
- [26] XIANG Teng-fei, ZHANG Min, SADIG H.R., LI Ze-cai, ZHANG Man-xin, DONG Chun-dong, YANG Ling, CHAN Wen-ming, LI Cheng. Slippery liquid-infused porous surface for corrosion protection with self-healing property [J]. Chemical Engineering Journal, 2018, 345: 147–155.
- [27] TUO Yan-jing, ZHANG Hai-feng, CHEN Wei-ping, LIU Xiao-wei Liu. Corrosion protection application of slippery liquid-infused porous surface based on aluminum foil [J]. Applied Surface Science, 2017, 423: 365–374.
- [28] XING Kai, LI Zhong-xu, WANG Zong-rong, QIAN Sun-xiang, FENG Jie, GU Chang-dong, TU Jiang-ping. Slippery coatings with mechanical robustness and self-replenishing properties as potential application on magnesium alloys [J]. Chemical Engineering Journal, 2021, 418: 129079.
- [29] CHEN Yan-ning, WU Liang, YAO Wen-hui, CHEN Yong-hua, ZHONG Zhi-yong, CI Wen-jun, WU Jia-hao, XIE Zhi-hui, YUAN Yuan, PAN Fu-sheng. A self-healing corrosion protection coating with graphene oxide carrying 8-hydroxyquinoline doped in layered double hydroxide on a micro-arc oxidation coating [J]. Corrosion Science, 2022, 194: 109941.
- [30] ZHANG Gen, WU Liang, TANG Ai-tao, WENG Bo, ATRENS A, MA Shi-da, LIU Lei Liu, PAN Fu-sheng. Sealing of anodized magnesium alloy AZ31 with MgAl layered double hydroxides layers [J]. RSC Advances, 2018, 8: 2248–2259.
- [31] ZHANG Guo-tao, SHI Ying-kang, TONG Bao-hong, JIAO Yun-long, YIN Yan-guo, LIU Kun. Exudation behavior and pinning effect of the droplet on slippery liquid-infused porous surfaces (SLIPS) [J]. Surface and Coatings Technology, 2022, 433: 128062.
- [32] ZHANG Gen, WU Liang, TANG Ai-tao, ZHANG Shuo, YUAN Bo, ZHENG Zhi-cheng, PAN Fu-sheng. A novel approach to fabricate protective layered double hydroxide films on the surface of anodized Mg–Al alloy [J]. Advanced Materials Interfaces, 2017, 4: 1700163.
- [33] NOVOSELOV K S, FALKO V I, COLOMBO L, GELLERT P R, SCHWAB M G, KIM K. A roadmap for graphene [J]. Nature, 2012, 490: 192–200.
- [34] PRASAI D, TUBERQUIA J C, HARL R R, JENNINGS G K, ROGERS B R, BOLOTIN K I. Graphene: Corrosion-inhibiting coating [J]. ACS Nano, 2012, 6: 1102–1108.
- [35] YAN Lu-chun, ZHOU Meng, PANG Xiao-lu, GAO Ke-wei. One-step in situ synthesis of reduced graphene oxide/Zn–Al layered double hydroxide film for enhanced corrosion protection of magnesium alloys [J]. Langmuir, 2019, 35: 6312–6320.

电解液 pH 值对镁合金表面灌注液体型光滑多孔表面耐腐蚀性能的影响

姚文辉^{1,2}, 詹国祥¹, 陈勇花¹, 秦洁¹, 吴量^{1,2},
陈燕宁¹, 吴嘉豪¹, 蒋斌^{1,2}, Andrej ATRENS³, 潘复生^{1,2}

1. 重庆大学 材料科学与工程学院, 重庆 400044;

2. 重庆大学 国家镁合金材料工程技术研究中心, 重庆 400044;

3. School of Mechanical and Mining Engineering, The University of Queensland, Brisbane Qld 4072, Australia

摘要: 在 AZ31 镁合金表面制备灌注液体型光滑多孔表面(SLIPS), 从而为镁合金提供腐蚀防护。将粗糙多孔的层状双金属氢氧化物(LDH)作为纳米容器, 用以盛放液体润滑液。通过调节电解液的 pH 值, 获得用于构筑 SLIPS 的最佳 LDH 膜层。研究不同 pH 值对 SLIPS 表面形貌、表面润湿性和电化学行为的影响规律。结果表明, 当 pH 值为 10.5 时, 所制备的 MgAl-LDH 膜层厚度最大, 为 3.51 μm , 其可盛放最多的硅油, 质量高达 0.22 mg/mm^2 , 使得该 MgAl-LDH 膜层所构筑的 SLIPS 可为镁合金提供最优的腐蚀防护性能, 腐蚀电流密度最低, 为 $3.72 \times 10^{-9} \text{ A}/\text{cm}^2$ 。另一方面, 与超疏水表面相比, 无论在电化学测试还是在长期浸泡试验中, SLIPS 均可作为 AZ31 镁合金基体提供更好的腐蚀防护。镁合金耐腐蚀性能的提高将进一步促进其在实践中的广泛应用。

关键词: 灌注液体型光滑多孔表面; 电解液 pH 值; 耐腐蚀性; 表面疏水性; AZ31 镁合金

(Edited by Xiang-qun LI)